Clinical Radiology 74 (2019) 437–444

Contents lists available at ScienceDirect

Clinical Radiology

journal homepage: www.clinicalradiologyonline.net

Evaluation of a newly developed 2D parametric parenchymal blood flow technique with an automated vessel suppression algorithm in patients with chronic thromboembolic pulmonary hypertension undergoing balloon pulmonary angioplasty

S.K. Maschke [a], H.M.B. Winther [a], T. Meine [a], T. Werncke [a], K.M. Olsson [b], M.M. Hoeper [b], J. Baumgart [c], F.K. Wacker [a], B.C. Meyer [a], J. Renne [a,1], J.B. Hinrichs [a,*,1]

[a] *Department of Diagnostic and Interventional Radiology, Member of the German Center for Lung Research (DZL), Hannover Medical School, Hannover, Germany*

[b] *Clinic for Pneumology, Member of the German Center for Lung Research (DZL), Hannover Medical School, Hannover, Germany*

[c] *Siemens Medical Solutions USA, Inc., Angiography, Fluoroscopic and Radiographic Systems, Hoffman Estates, IL, USA*

ARTICLE INFORMATION

Article history:
Received 23 October 2018
Accepted 3 December 2018

AIM: To evaluate the feasibility of two-dimensional parametric parenchymal blood flow (2D-PPBF) to quantify perfusion changes in the lung parenchyma following balloon pulmonary angioplasty (BPA) for treatment of chronic thromboembolic pulmonary hypertension.

MATERIALS AND METHODS: Overall, 35 consecutive interventions in 18 patients with 98 treated pulmonary arteries were included. To quantify changes in pulmonary blood flow using 2D-PPBF, the acquired digital subtraction angiography (DSA) series were post-processed using dedicated software. A reference region of interest (ROI; arterial inflow) in the treated pulmonary artery and a distal target ROI, including the whole lung parenchyma distal to the targeted stenosis, were placed in corresponding areas on DSA pre- and post-BPA. Half-peak density (HPD), wash-in rate (WIR), arrival to peak (AP), area under the curve (AUC), and mean transit time (MTT) were assessed. The ratios of the reference ROI to the target ROI ($HPD_{parenchyma}/HPD_{inflow}$, $WIR_{parenchyma}/WIR_{inflow}$; $AP_{parenchyma}/AP_{inflow}$, $AUC_{parenchyma}/AUC_{inflow}$, $MTT_{parenchyma}/MTT_{inflow}$) were calculated. The relative differences of the 2D-PPBF parameters were correlated to changes in the pulmonary flow grade score.

RESULTS: The pulmonary flow grade score improved significantly after BPA (1 versus 3; $p<0.0001$). Likewise, the mean $HPD_{parenchyma}/HPD_{inflow}$ (−10.2%; $p<0.0001$), $AP_{parenchyma}/AP_{inflow}$ (−24.4%; $p=0.0007$), and $MTT_{parenchyma}/MTT_{inflow}$ (−3.5%; $p=0.0449$) decreased

* Guarantor and correspondent: J. B. Hinrichs, Institute for Diagnostic and Interventional Radiology, Hannover Medical School, Carl-Neuberg-Str. 1, 30625 Hannover, Germany. Tel.: +49 (511) 532 3421; fax: +49 (511) 532 9421.
E-mail address: hinrichs.jan@mh-hannover.de (J.B. Hinrichs).

[1] These authors contributed equally to the manuscript.

https://doi.org/10.1016/j.crad.2018.12.023

significantly, whereas $WIR_{parenchyma}/WIR_{inflow}$ (+82.4%) and $AUC_{parenchyma}/AUC_{inflow}$ (+58.6%) showed a significant increase ($p<0.0001$). Furthermore, a significant correlation between changes of the pulmonary flow grade score and changes of $HPD_{parenchyma}/HPD_{inflow}$ ($\rho=-0.21$, $p=0.04$), $WIR_{parenchyma}/WIR_{inflow}$ ($\rho=0.43$, $p<0.0001$), $AP_{parenchyma}/AP_{inflow}$ ($\rho=-0.22$, $p=0.03$), $AUC_{parenchyma}/AUC_{inflow}$ ($\rho=0.48$, $p<0.0001$), and $MTT_{parenchyma}/MTT_{inflow}$ ($\rho=-0.39$, $p<0.0001$) could be observed.

CONCLUSION: The 2D-PPBF technique is feasible for the quantification of perfusion changes following BPA and has the potential to improve monitoring of BPA.

Introduction

Chronic thromboembolic pulmonary hypertension (CTEPH) is a life-threatening but potentially curable form of pulmonary hypertension caused by persistent obstruction of pulmonary arteries as a result of residual pulmonary emboli and intraluminal post-embolic scar-tissue strictures.[1,2] The prevalence of CTEPH is reported to be 0.1–4% in pulmonary embolism survivors.[1,3–6] The median survival of patients with untreated CTEPH and mean pulmonary artery pressure (mPAP) of >30 mmHg is <2 years.[7,8] Treatment of choice for CTEPH is pulmonary endarterectomy (PEA) with a reported perioperative mortality of 2–4% and strong scientific evidence for improved patient outcome[1,9]; however, up to 50% of patients are not suitable for surgery, mostly due to distal and therefore inaccessible thromboembolic material.[4,6,10,11] Besides medical therapies (e.g., riociguat, macitentan, sildenafil, or tadalafil), balloon pulmonary angioplasty (BPA) is a treatment option for inoperable patients, addressing peripheral web-like stenosis and intraluminal bands in segmental and sub-segmental pulmonary arteries as well as total occlusions.[12] Improvements in haemodynamics and clinical symptoms are reported following BPA.[13–19] In recent years, BPA has been refined and optimised in order to increase the therapeutic effect and to avoid potentially life-threatening complications.[12,20–24] Nevertheless, clear procedural endpoints following BPA are still missing.

2D parametric parenchymal blood flow (2D-PPBF) is a further development of known techniques for the quantification of tissue perfusion based on dedicated post-processing of regular digital subtraction angiography (DSA) images.[25–27] The potential value of perfusion measurements during and after interventional procedures has already been described in a wide range of vascular interventions using different ROI sizes[25–31]; however, when intending to measure tissue perfusion the signal from the greater vessels needs to be excluded from the analysis. Due to further developments of the currently available 2D-PPBF technique, the greater vessels can be automatically suppressed by a new software algorithm, allowing the use of large target ROIs covering all of the parenchyma behind a treated lesion. It was hypothesised that the new 2D-PPBF technique has the potential to assess tissue perfusion of the whole lung parenchyma behind a treated CTEPH lesion and thus may be more comprehensive compared to the established pulmonary flow grade score.[32] Therefore, the purpose of the present study was to evaluate the feasibility of 2D-PPBF to quantify perfusion changes of the whole lung parenchyma distal to a CTEPH lesion following BPA.

Material and methods

This retrospective study was approved by the local ethics committee. According to current guidelines, all patients underwent a standardised diagnostic CTEPH work-up and treatment decision was reached by an inter-disciplinary CTEPH board.[33] Eighteen patients (11 females, seven males; mean age 64.8±9.9 years) with CTEPH (mPAP 45±18.4 mmHg) scheduled for BPA were included in the study. Between November 2016 and November 2017 these patients underwent 35 consecutive BPA procedures for the treatment of 98 pulmonary artery segments. The enrolled patients were treated with targeted drugs for pulmonary hypertension, such as riociguat, macitentan, sildenafil, or tadalafil, and received appropriate anticoagulation. No patient had to be excluded from the analysis.

BPA

Anticoagulation was stopped for the day of the intervention. All procedures were performed on a monoplane, ceiling-mounted angiographic system (Artis Q, Siemens Healthcare, Forchheim, Germany) or on a monoplane, robotic-arm-mounted angiographic system (Artis pheno, Siemens Healthcare) under local anaesthesia and by use of C-arm computed tomography (CACT) guidance.[12] Lesions were identified on selective CACT. A long 6 F sheath (Destination peripheral guiding sheath, Terumo Europe, Leuven, Belgium) was placed in the main pulmonary artery of interest via femoral access. Afterwards, a 6 F guiding catheter (MACH 1, Boston Scientific, Marlborough, MA, USA) was advanced next to the targeted pulmonary artery segment and a 0.014-inch guidewire (V-14, Boston Scientific) was used to cross the target lesion. Thereafter, appropriate rapid-exchange balloon catheters (1.2–4 mm, Emerge, Boston Scientific; based on CACT) were forwarded to dilate the target lesion. DSA undertaken with manual

contrast medium injections were acquired pre- and post-BPA at 4 frames/s and with a range of 10–30 seconds in modest inspiratory breath-hold. The pre- and post-interventional DSA images were acquired in the same projection and with comparable catheter positions.

The perfusion changes following each BPA procedure were evaluated with the commonly used and visually based pulmonary flow grade score as described by Inami *et al.*[32] To determine the flow appearance and flow grade following BPA, selective angiograms of the treated vessels were performed through catheters engaged near the treated vessels.[32] These were graded 0–3: grade 0 = no or minimal perfusion behind the target lesion; grade 1 = partial perfusion of the segmental pulmonary arteries; grade 2 = complete perfusion of the segmental pulmonary arteries and partial perfusion of the pulmonary veins; grade 3 = complete perfusion of arterial and venous pulmonary vessels. The end-point for BPA was the maximum achievable increase in the pulmonary flow grade score using an appropriately undersized balloon.

Image analysis

The angiographic datasets were post-processed on a dedicated workstation (syngo X Workplace VD20B, Siemens Healthcare). Post-processing was done with a newly developed 2D-PPBF prototype technique capable of excluding the signal of larger vessels from analysis. The motion-corrected DSA frames were filtered with a band-reject filter tuned to suppress the vessels. The resulting images were then used to visualise and analyse parenchymal flow without the strong presence of vessels (US Patent 8,848,996). Two radiologists (blinded) agreed upon ROI placement in consensus, i.e., one proximal to the vascular lesion in the targeted pulmonary artery in order to assess the arterial inflow, and another distal to the treated lesion including the lung parenchyma. The circular inflow ROIs were placed directly distal to the tip of the guiding catheter as a reference point guaranteed to have contrast.[29] The target ROIs were drawn freehand alongside the sub-/segmental boundaries, including the complete lung parenchyma distal to the intervened lesion. All ROIs were copied to the corresponding images acquired after BPA in order to ensure that in both images ROIs were placed in the same position (Fig 1; illustrative example of ROI placement). Numeric density values for half peak density (HPD), wash-in rate (WIR), arrival to peak (AP), area under the curve (AUC) and mean transit time (MTT) were recorded (Table 1; Fig 2). The HPD represents the time from the start of the angiographic run to half the maximum density within the target ROI; the WIR describes the rate at which contrast increases from arrival of contrast medium in the ROI to peak density; AP comprises the time from arrival of contrast medium in the ROI until peak density is reached; AUC indicates the density values in a single ROI throughout the entire angiographic run; and MTT describes the duration of elevated signal intensity in the ROI as measured by arrival of contrast medium to the ROI from the centre of gravity of the time–density curve, estimating the time the blood spends in the parenchymal circulation. The ratios of the reference to the target ROI ($HPD_{parenchyma}/HPD_{inflow}$, $WIR_{parenchyma}/WIR_{inflow}$, $AP_{parenchyma}/AP_{inflow}$, $AUC_{parenchyma}/AUC_{inflow}$, $MTT_{parenchyma}/MTT_{inflow}$) pre- and post-BPA were calculated. The changes the 2D-PPBF parameters were correlated to changes in the pulmonary flow grade score following BPA. The pulmonary flow grade score was assessed by two radiologists (blinded) in consensus, with an interval of 4 weeks from the 2D-PPBF measurements and in random order.

Statistical analysis

Descriptive statistical analyses of angiographic data and the patient demographics were calculated. The 2D-PPBF values are presented as mean ± standard deviation (SD). Values of the pulmonary flow grade score are given as median with minimum and maximum value. Comparisons between pre- and post-intervention data were made using a pairwise Wilcoxon signed-rank test. The differences in pre- and post-BPA, 2D-PPBF data were analysed and correlated to changes in the pulmonary flow grade score using Spearman's rank correlation coefficient (ρ). A p-value <0.05 was defined as statistically significant. Statistical analyses were conducted using commercially available software (JMP 12, SAS Institute, JMP Office Germany, Böblingen, Germany).

Results

Overall, 35 consecutive BPA procedures (right lung 19 [54.3%] and left lung 16 [45.7%]) in 18 patients were analysed in this study. On average 3±2 segmental or subsegmental pulmonary arteries were treated per BPA procedure. In the right lung, BPAs of 48 pulmonary arteries (upper lobe n=15 [31.2%]; middle lobe n=9 [18.8%]; lower lobe n=24 [50%]) and in the left lung BPAs of 49 pulmonary arteries (upper lobe n=32 [65.3%]; lower lobe n=17 [34.7%]) were performed.

The pulmonary flow grade score improved significantly from grade 1 (1; 2) to grade 3 (2; 3) ($p<0.0001$). In the pre- and post-interventional 2D-PPBF comparison, the mean $HPD_{parenchyma}/HPD_{inflow}$ (−10.2%; $p<0.0001$) as well as $AP_{parenchyma}/AP_{inflow}$ (−24.4%; $p=0.0007$) and $MTT_{parenchyma}/MTT_{inflow}$ (−3.5%; $p=0.0449$) decreased significantly whereas $WIR_{parenchyma}/WIR_{inflow}$ showed a significant increase of 82.4% ($p<0.0001$). Likewise, $AUC_{parenchyma}/AUC_{inflow}$ increased by 58.6% ($p<0.0001$). The treatment results are summarised in Table 2, and an example of 2D-PPBF is shown in Fig 3.

The analysis of changes (Δ) in the pulmonary flow grade score, $HPD_{parenchyma}/HPD_{inflow}$, $WIR_{parenchyma}/WIR_{inflow}$, $AP_{parenchyma}/AP_{inflow}$, $AUC_{parenchyma}/AUC_{inflow}$, and $MTT_{parenchyma}/MTT_{inflow}$ due to BPA, showed a significant association between Δpulmonary flow grade score and $\Delta HPD_{parenchyma}/HPD_{inflow}$ ($\rho=-0.21$, $p=0.04$), $\Delta WIR_{parenchyma}/WIR_{inflow}$ ($\rho=0.43$, $p<0.0001$), $\Delta AP_{parenchyma}/AP_{inflow}$ ($\rho=-0.22$, $p=0.03$), $\Delta AUC_{parenchyma}/AUC_{inflow}$ ($\rho=0.48$, $p<0.0001$) and $\Delta MTT_{parenchyma}/MTT_{inflow}$ ($\rho=-0.39$, $p<0.0001$).

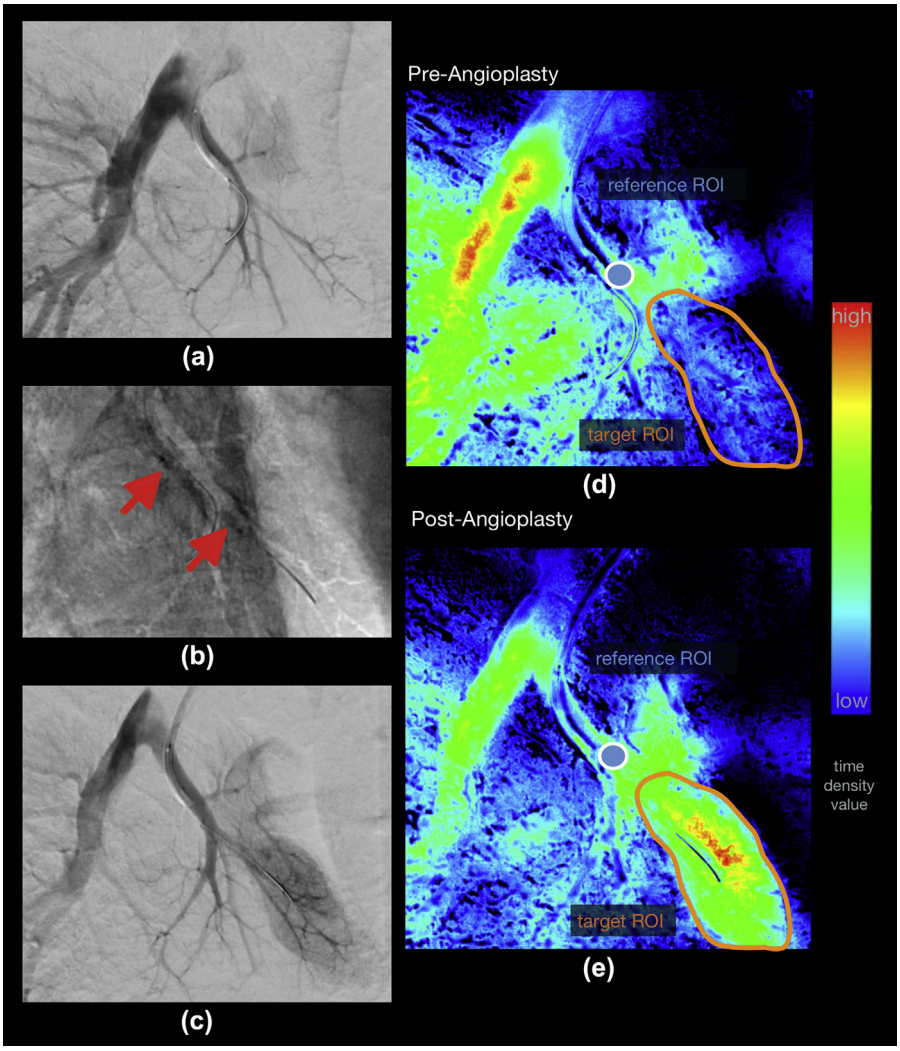

Figure 1 Example of ROI placement pre- and post-intervention. Shown are images of a 63-year-old female patient with CTEPH, who underwent BPA in a lower lobe segmental artery of the right lung. DSA pre- (a) and post-BPA (c) and corresponding 2D-PPBF images (d,e) are presented. (b) The inflated balloon dilating the target lesion (red arrows). The reference ROI (blue) is positioned within the proximal segmental artery distal to the tip of the guiding catheter, while the target ROI (orange) is placed distally with full coverage of the lung parenchyma distal to the treated lesion. The time–density value is colour encoded.

Table 1
Perfusion parameter descriptions.

AP	arrival to peak = time from contrast medium arrival in the region of interest (ROI) until it first reaches maximum density
AUC	area under the curve = density values in a single ROI throughout the entire angiographic run; representing the total contrast intensity across time
BAT	bolus arrival time = the time from the beginning of the contrast medium injection until it reaches 20% of maximum intensity in the ROI
COG	center of gravity = point at which time and density are evenly dispersed
HPD	half peak density = time that contrast intensity reaches half of the maximum in the target ROI
MTT	mean transit time = duration of elevated signal intensity in the ROI as measured by arrival of contrast medium to the ROI from the centre of gravity of the time–density curve; estimating the time the blood spends in the parenchymal circulation
WIR	wash-in rate = rate at which contrast increases in the ROI from arrival to peak density

Discussion

The present retrospective study investigated the feasibility of a newly developed 2D-PPBF technique, which suppresses the signal of the greater vessels from the analysis to obtain pure depiction of lung tissue perfusion, for evaluation and quantification of perfusion changes in the lung parenchyma distal to CTEPH lesions treated by BPA.

The 2D-PPBF parameters were compared to the pulmonary flow grade score, a well-established, visually assessed parameter used to analyse perfusion changes of the lung parenchyma due to BPA.[32] As expected, the pulmonary flow grade score improved significantly after BPA. Likewise, perfusion parameters ($HPD_{parenchyma}/HPD_{inflow}$, $WIR_{parenchyma}/WIR_{inflow}$, $AP_{parenchyma}/AP_{inflow}$, $AUC_{parenchyma}/AUC_{inflow}$, $MTT_{parenchyma}/MTT_{inflow}$) showed corresponding and significant changes following BPA. Additionally,

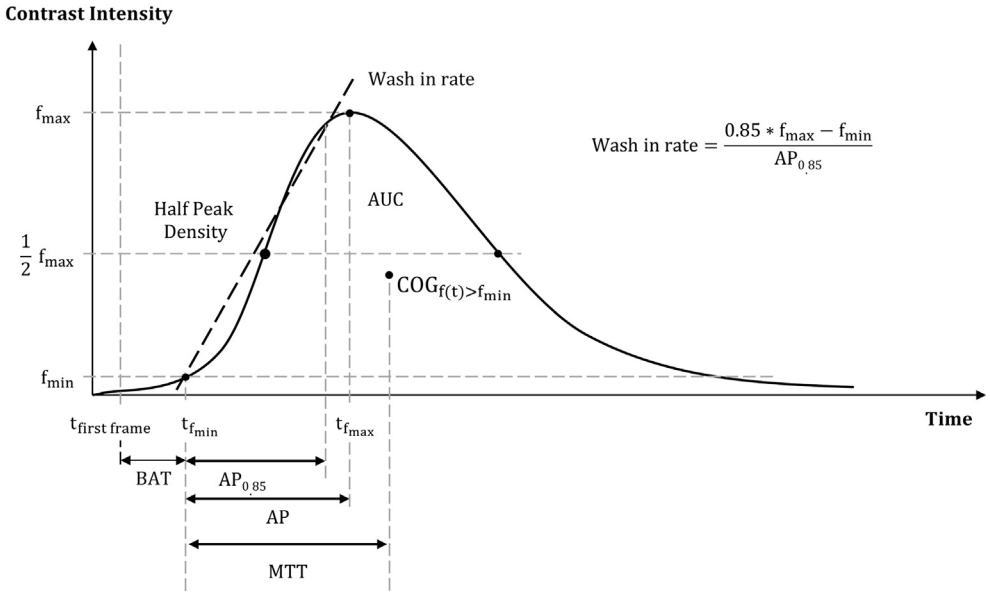

Figure 2 Idealised example of a time–density curve describing the flow of contrast agent over time in the defined region of interest. Wash in rate is measured to 85% of peak to better assess the ascending slope of the curve and to minimise influence of a plateau of the curve before the peak density is reached. AUC = area under the curve, AP = arrival to peak, BAT = bolus arrival time, COG = centre of gravity, MTT = mean transit time.

Δpulmonary flow grade score showed a significant association to $\Delta HPD_{parenchyma}/HPD_{inflow}$, $\Delta AP_{parenchyma}/AP_{inflow}$, $\Delta AUC_{parenchyma}/AUC_{inflow}$, and $\Delta MTT_{parenchyma}/MTT_{inflow}$. Taken together, these findings emphasise the assumption that BPA leads to an increased pulmonary blood flow and parenchymal perfusion. To date, perfusion assessment during a broad variety of angiographic interventions is primarily based on commonly used iodinated contrast angiography, and therefore, as it depends on visual assessment of arterial flow, is highly subjective and operator depended, and subsequently, shows significant interobserver and intra-observer variation.[28,34,35] In BPA, the accepted pulmonary flow grade score, has the same limitations as it is also a visually based and thus highly subjective parameter[32]; however, as shown previously, 2D perfusion angiography bares the potential to assess objective information regarding perfusion changes in angiographic interventions as, similar to other imaging techniques such as magnetic resonance imaging (MRI) or computed tomography (CT), it assigns density values to each area with a defined ROI.[36,37] The calculated mean density values for the ROI in each frame can be used to generate objective information regarding flow time, maximal values, and rates of flow.[26] Additionally, the independence of 2D perfusion angiography measurements from fixed pump injections, which is mandatory in BPA to avoid severe injuries of the small and vulnerable pulmonary vessels, has been demonstrated before.[27,29,31] Conventional 2D perfusion angiography is used to quantitatively assess perfusion changes of the lung parenchyma following BPA[29]; however, the technique used in the former study was not able to exclude greater vessels from the analysis. Therefore, relatively small target ROIs were used to avoid an adulteration by superimposition of great pulmonary arteries and veins.[29] The use of small ROIs restricted the measurements to small representative areas of the lung parenchyma behind the treated lesion without the ability to analyse the whole treated segment within one ROI. 2D-PPBF was developed to overcome this issue. This technique is capable of calculating 2D-PPBF images by automatically suppressing greater vessels and, therefore, only depicting parenchymal perfusion. Therefore, 2D-PPBF allows the inclusion of the whole lung parenchyma distal to the treated pulmonary artery as one target ROI and, thus, offers a more precise and

Table 2
Changes in pulmonary flow grade score and 2D parametric parenchymal blood flow after BPA.

	Pre-Intervention	Post-Intervention	Difference (%)	*p*-Value
Pulmonary flow grade score	1 (1; 2)	3 (2; 3)	/	<0.0001
$HPD_{parenchyma}/HPD_{inflow}$	1.57±0.39 [1.5; 1.65]	1.41±0.36 [1.33; 1.48]	−0.16 (10.2%)	<0.0001
$WIR_{parenchyma}/WIR_{inflow}$	0.17±0.19 [0.13; 0.2]	0.31±0.26 [0.25; 0.36]	+0.14 (82.4%)	<0.0001
$AP_{parenchyma}/AP_{inflow}$	2.46±2.0 [2.1; 2.9]	1.86±1.74 [1.51; 2.21]	−0.6 (24.4%)	0.0007
$AUC_{parenchyma}/AUC_{inflow}$	0.29±0.19 [0.24; 0.32]	0.46±0.24 [0.41; 0.51]	+0.17 (58.6%)	<0.0001
$MTT_{parenchyma}/MTT_{inflow}$	1.44±0.26 [1.39; 1.49]	1.39±0.25 [1.34; 1.44]	−0.05 (3.5%)	0.0449

Pulmonary flow grade score and 2D parametric parenchymal blood flow values were assessed for each treated segmental pulmonary artery. Median values (minimum; maximum) are given for the pulmonary flow grade score; mean values±standard deviation [95% confidence intervals] and percent difference between pre- and post-intervention are given for the 2D parametric parenchymal blood flow values. Comparison of pre- and post-intervention values was done by pairwise Wilcoxon signed-rank test.
AP, arrival to peak; AUC, area under the curve; HPD, half peak density; MTT, mean transit time; WIR, wash-in rate.

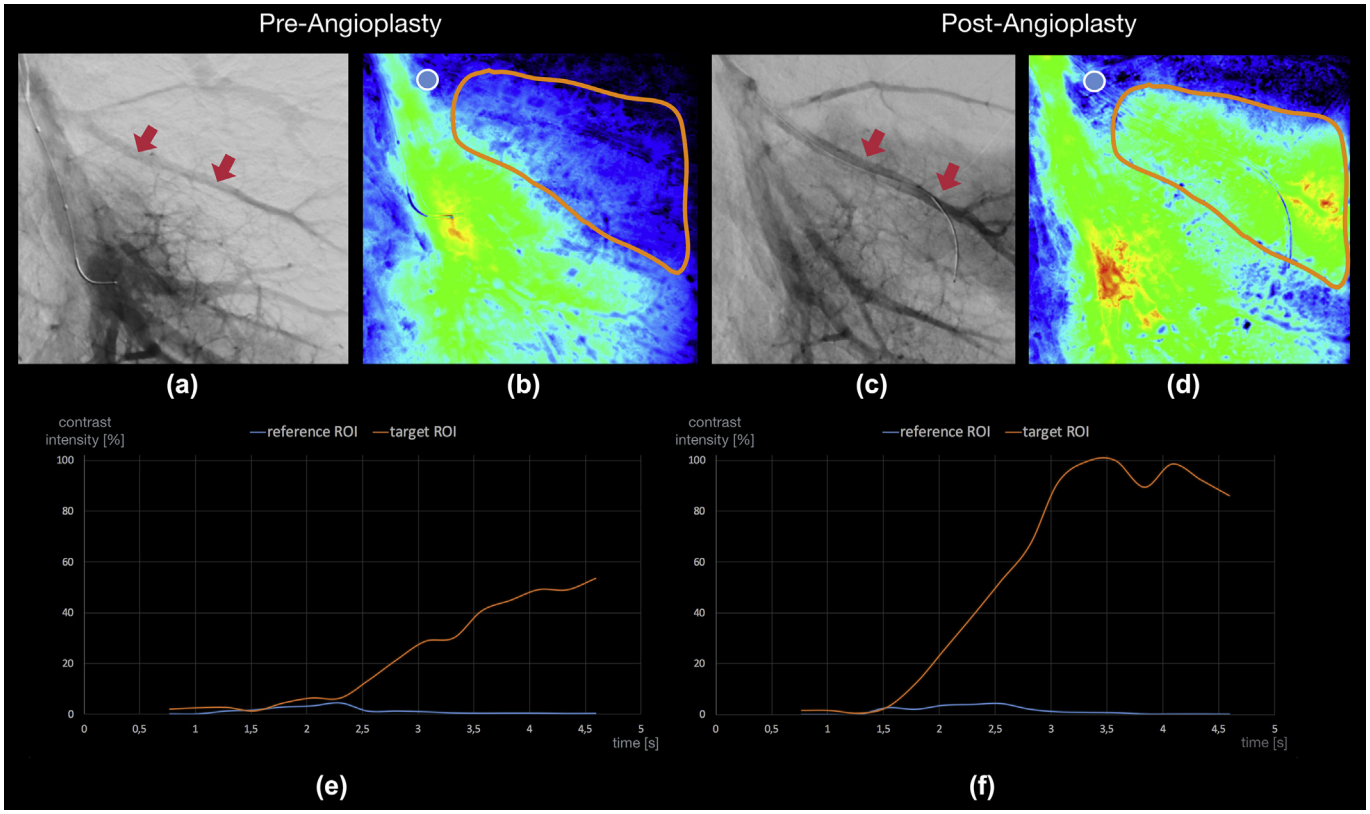

Figure 3 Example of 2D-PPBF pre- and post-BPA. In this 66-year-old male patient with CTEPH a left lower lobe segmental artery was treated. (a) Red arrows in this angiography series mark a sub-segmental artery with reduced flow due to proximal web stenosis, resulting in (b) low parenchymal time–density values in the dependent areas, (e) prolonged time to peak within the parenchyma and a low AUC. (c) After angioplasty improved flow within the same sub-segmental artery (red arrows) led to (d) increased parenchymal time–density values and a shorter time to peak value as well as a higher area under the curve within the target ROI (f).

comprehensive analysis of tissue perfusion. Moreover, the new 2D-PPBF technique is comparable to established techniques for visualisation of acute pulmonary embolism using CT perfusion imaging, also requiring vessel removal prior to reliable data analysis.[38]

Furthermore, additional 2D-PPBF parameters were evaluated to obtain a more detailed perfusion analysis based on more extensive curve sketching of the calculated time–density curves. In previous studies, the described perfusion parameters primarily offered basic information regarding the flow of contrast, including the time to peak and peak density[25–29,31]; however, the time–density curves calculated within 2D-PPBF contain more detailed information regarding the flow of contrast medium than has been exploited before, offering a continuative analysis that has the potential to monitor perfusion changes during angiographic interventions more comprehensively.[35] Hereby, MTT, as it likewise takes blood inflow and outflow into account, might be of particular importance regarding evaluation of interventional success and patient outcome, as it has been proven to be a valuable predictor of both outcome in acute stroke and appearance of subsequent stroke in symptomatic carotid occlusion,[39,40] emphasising its predictive value. Moreover, the other evaluated parameters, HPD, WIR, AP, and AUC have also been demonstrated to offer reliable information regarding characterisation of tissue perfusion in different modalities and diseases, promising new perspectives of clinical diagnostic and prediction of outcome.[41,42] Altogether, 2D-PPBF offers a feasible approach to analyse perfusion changes following BPA in detail with the clinical perspective to improve periprocedural monitoring and management and, thus, increase therapeutic benefit. Furthermore, 2D-PPBF has the potential to serve as a novel quantitative imaging parameter to define possible end-points and the technical success of BPA procedures.

Movement is reported to hinder precise measurements of 2D-perfusion angiography during endovascular treatment of peripheral arterial disease when analysing tissue perfusion of the foot or when analysing perfusion changes following transarterial chemoembolisation.[25,26,28,43] At Hannover Medical School, image acquisition and catheterisation during BPA procedures is performed by the use of short, reproducible inspiratory breath-holds. Therefore, except for cardiac motion, movement artefacts are controlled and reduced to a minimum. Cardiac motion is mostly constant during the intervention and thus, comparable effects caused by cardiac motion should influence DSA runs pre- and post-BPA and may, therefore, be negligible.[29]

Limitations

This study included a relatively small number of patients undergoing BPA at a single institution. Long-term follow-up of patient outcome was not part of this analysis. The final end-point for successful revascularisation following BPA is clinical improvement, which is determined after multiple BPA sessions. Therefore, a meaningful evaluation of clinical improvements after one single BPA is hard to assess and usually not performed. To further assess the usefulness of 2D-PPBF and to determine possible, 2D-PPBF based end-points for BPA, a multicentric study with larger study population and complete long-term follow-up is necessary. Another limitation is the comparison of 2D-PPBF to the pulmonary flow grade score. The pulmonary flow grade score is a subjective measurement with room for user-dependent interpretations. Nevertheless, this score is widely and commonly used and up to date without a real alternative when assessing the therapeutic success during the intervention. Pressure wire measurements might help to overcome the issue of a missing objective parameter to monitor BPA; however, this adds cost and complexity to an already challenging procedure, but may be of high value to evaluate the true benefit of 2D-PPBF.

In conclusion, the evaluated new 2D-PA technique is feasible for the quantification of perfusion changes following BPA and has the potential to improve monitoring of BPA in the interventional suite.

Conflict of interest

The authors declare no conflict of interest.

Acknowledgements

The study was funded in parts by personal grants from Hannover Medical School ("Junge Akademie" Program) and by institutional grants from the German Centre of Lung Research (DZL/BREATH). The authors of this manuscript declare relationships with the following companies: Siemens Healthcare and ProMedicus (B.C.M. and F.K.W.; outside the submitted work); Bayer (M.M.H. and K.M.O.; outside the submitted work). J.B. has a patent (US Patent 8848996) issued. The remaining authors declare no relationships with any companies whose products or services may be related to the subject matter of the article.

References

1. Hoeper MM, Madani MM, Nakanishi N, *et al*. Chronic thromboembolic pulmonary hypertension. *Lancet Respir Med* 2014;**2**:573–82.
2. Poch DS, Auger WR. Chronic thromboembolic pulmonary hypertension: detection, medical and surgical treatment approach, and current outcomes. *Heart Fail Rev* 2016;**21**:309–22.
3. Guérin L, Couturaud F, Parent F, *et al*. Prevalence of chronic thromboembolic pulmonary hypertension after acute pulmonary embolism. *Thromb Haemost* 2014;**112**:598–605.
4. Kramm T, Wilkens H, Fuge J, *et al*. Incidence and characteristics of chronic thromboembolic pulmonary hypertension in Germany. *Clin Res Cardiol* 2018;**130**:508.
5. Coquoz N, Weilenmann D, Stolz D, *et al*. Multicentre observational screening survey for the detection of CTEPH following pulmonary embolism. *Eur Respir J* 2018;**51**:1702505.
6. Pepke-Zaba J, Delcroix M, Lang I, *et al*. Chronic thromboembolic pulmonary hypertension (CTEPH): results from an international prospective registry. *Circulation* 2011;**124**:1973–81.
7. Delcroix M, Lang I, Pepke-Zaba J, *et al*. Long-term outcome of patients with chronic thromboembolic pulmonary hypertension: results from an international prospective registry. *Circulation* 2016;**133**:859–71.
8. Lewczuk J, Piszko P, Jagas J, *et al*. Prognostic factors in medically treated patients with chronic pulmonary embolism. *Chest* 2001;**119**:818–23.
9. Cannon JE, Su L, Kiely DG, *et al*. Dynamic risk stratification of patient long-term outcome after pulmonary endarterectomy: results from the United Kingdom National Cohort. *Circulation* 2016;**133**:1761–71.
10. Madani MM, Auger WR, Pretorius V, *et al*. Pulmonary endarterectomy: recent changes in a single institution's experience of more than 2,700 patients. *Ann Thorac Surg* 2012;**94**:97–103. Discussion 103.
11. Jenkins DP, Madani M, Mayer E, *et al*. Surgical treatment of chronic thromboembolic pulmonary hypertension. *Eur Respir J* 2013;**41**:735–42.
12. Hinrichs JB, Renne J, Hoeper MM, *et al*. Balloon pulmonary angioplasty: applicability of C-arm CT for procedure guidance. *Eur Radiol* 2016;**26**:4064–71.
13. Feinstein JA, Goldhaber SZ, Lock JE, *et al*. Balloon pulmonary angioplasty for treatment of chronic thromboembolic pulmonary hypertension. *Circulation* 2001;**103**:10–3.
14. Kataoka M, Inami T, Hayashida K, *et al*. Percutaneous transluminal pulmonary angioplasty for the treatment of chronic thromboembolic pulmonary hypertension. *Circ Cardiovasc Interv* 2012;**5**:756–62.
15. Mizoguchi H, Ogawa A, Munemasa M, *et al*. Refined balloon pulmonary angioplasty for inoperable patients with chronic thromboembolic pulmonary hypertension. *Circ Cardiovasc Interv* 2012;**5**:748–55.
16. Sugimura K, Fukumoto Y, Satoh K, *et al*. Percutaneous transluminal pulmonary angioplasty markedly improves pulmonary hemodynamics and long-term prognosis in patients with chronic thromboembolic pulmonary hypertension. *Circ J* 2012;**76**:485–8.
17. Andreassen AK, Ragnarsson A, Gude E, *et al*. Balloon pulmonary angioplasty in patients with inoperable chronic thromboembolic pulmonary hypertension. *Heart* 2013;**99**:1415–20.
18. Fukui S, Ogo T, Morita Y, *et al*. Right ventricular reverse remodelling after balloon pulmonary angioplasty. *Eur Respir J* 2014;**43**:1394–402.
19. Olsson KM, Wiedenroth CB, Kamp J-C, *et al*. Balloon pulmonary angioplasty for inoperable patients with chronic thromboembolic pulmonary hypertension: the initial German experience. *Eur Respir J* 2017;**49**:1602409.
20. Roik M, Wretowski D, Łabyk A, *et al*. Refined balloon pulmonary angioplasty driven by combined assessment of intra-arterial anatomy and physiology—multimodal approach to treated lesions in patients with non-operable distal chronic thromboembolic pulmonary hypertension — technique, safety and efficacy of 50 consecutive angioplasties. *Int J Cardiol* 2016;**203**:228–35.
21. Roik M, Wretowski D, Labyk A, *et al*. Optical coherence tomography imaging of inoperable chronic thromboembolic pulmonary hypertension treated with refined balloon pulmonary angioplasty. *Pol Arch Med Wewn* 2014;**124**:742–3.
22. Bouvaist H, Thony F, Jondot M, *et al*. Balloon pulmonary angioplasty in a patient with chronic thromboembolic pulmonary hypertension. *Eur Respir Rev* 2014;**23**:393–5.
23. Inohara T, Kawakami T, Kataoka M, *et al*. Lesion morphological classification by OCT to predict therapeutic efficacy after balloon pulmonary angioplasty in CTEPH. *Int J Cardiol* 2015;**197**:23–5.
24. Inami T, Kataoka M, Shimura N, *et al*. Pressure-wire-guided percutaneous transluminal pulmonary angioplasty: a breakthrough in catheter-interventional therapy for chronic thromboembolic pulmonary hypertension. *JACC Cardiovasc Interv* 2014;**7**:1297–306.
25. Jens S, Marquering HA, Koelemay MJW, *et al*. Perfusion angiography of the foot in patients with critical limb ischemia: description of the technique. *Cardiovasc Intervent Radiol* 2015;**38**:201–5.
26. Murray T, Rodt T, Lee MJ. Two-dimensional perfusion angiography of the foot: technical considerations and initial analysis. *J Endovasc Ther* 2016;**23**:58–64.
27. Hinrichs JB, Murray T, Akin M, *et al*. Evaluation of a novel 2D perfusion angiography technique independent of pump injections for assessment

of interventional treatment of peripheral vascular disease. *Int J Cardiovasc Imaging* 2017;**33**:295–301.
28. Wang J, Cheng J-J, Huang K-Y, *et al*. Quantitative assessment of angiographic perfusion reduction using color-coded digital subtraction angiography during transarterial chemoembolization. *Abdom Radiol (NY)* 2016;**41**:545–52.
29. Maschke SK, Renne J, Werncke T, *et al*. Chronic thromboembolic pulmonary hypertension: evaluation of 2D-perfusion angiography in patients who undergo balloon pulmonary angioplasty. *Eur Radiol* 2017;**27**:4264–70.
30. Maschke SK, Werncke T, Klöckner R, *et al*. Quantification of perfusion reduction by using 2D-perfusion angiography following transarterial chemoembolization with drug-eluting beads. *Abdom Radiol (NY)* 2017;**65**:87–9.
31. Maschke SK, Werncke T, Renne J, *et al*. Transjugular intrahepatic portosystemic shunt (TIPS) dysfunction: quantitative assessment of flow and perfusion changes using 2D-perfusion angiography following shunt revision. *Abdom Radiol (NY)* 2018:1–8.
32. Inami T, Kataoka M, Shimura N, *et al*. Pulmonary edema predictive scoring index (PEPSI), a new index to predict risk of reperfusion pulmonary edema and improvement of hemodynamics in percutaneous transluminal pulmonary angioplasty. *JACC Cardiovasc Interv* 2013;**6**:725–36.
33. Hinrichs JB, Marquardt S, Falck von C, *et al*. Comparison of C-arm computed tomography and digital subtraction angiography in patients with chronic thromboembolic pulmonary hypertension. *Cardiovasc Intervent Radiol* 2016;**39**:53–63.
34. Reekers JA, Koelemay MJW, Marquering HA, *et al*. Functional imaging of the foot with perfusion angiography in critical limb ischemia. *Cardiovasc Intervent Radiol* 2016;**39**:183–9.
35. Kim AH, Shevitz AJ, Morrow KL, *et al*. Characterizing tissue perfusion after lower extremity intervention using two-dimensional color-coded digital subtraction angiography. *J Vasc Surg* 2017;**66**:1464–72.
36. Baradaran H, Fodera V, Mir D, *et al*. Evaluating CT perfusion deficits in global cerebral edema after aneurysmal subarachnoid hemorrhage. *AJNR Am J Neuroradiol* 2015;**36**:1431–5.
37. Schoenfeld C, Cebotari S, Hinrichs J, *et al*. MR Imaging-derived Regional Pulmonary Parenchymal Perfusion and Cardiac Function for Monitoring Patients with Chronic Thromboembolic Pulmonary Hypertension before and after Pulmonary Endarterectomy. *Radiology* 2016;**279**:925–34. https://doi.org/10.1148/radiol.2015150765.
38. Wildberger JE, Klotz E, Ditt H, *et al*. Multislice computed tomography perfusion imaging for visualization of acute pulmonary embolism: animal experience. *Eur Radiol* 2005;**15**:1378–86.
39. Grubb RL, Derdeyn CP, Videen TO, *et al*. Relative mean transit time predicts subsequent stroke in symptomatic carotid occlusion. *J Stroke Cerebrovasc Dis* 2016;**25**:1421–4.
40. Kamalian S, Kamalian S, Konstas AA, *et al*. CT perfusion mean transit time maps optimally distinguish benign oligemia from true “at-risk” ischemic penumbra, but thresholds vary by postprocessing technique. *AJNR Am J Neuroradiol* 2012;**33**:545–9.
41. Gu F, Han L, Yang X, *et al*. Value of time–intensity curve analysis of contrast-enhanced ultrasound in the differential diagnosis of thyroid nodules. *Eur J Radiol* 2018;**105**:182–7.
42. Cantisani V, Bertolotto M, Weskott HP, *et al*. Growing indications for CEUS: the kidney, testis, lymph nodes, thyroid, prostate, and small bowel. *Eur J Radiol* 2015;**84**:1675–84.
43. Lin Y-Y, Lee R-C, Guo W-Y, *et al*. Quantitative real-time fluoroscopy analysis on measurement of the hepatic arterial flow during transcatheter arterial chemoembolisation of hepatocellular carcinoma: comparison with quantitative digital subtraction angiography analysis. *Cardiovasc Intervent Radiol* 2016;**39**:1557–63.